THE JOURNAL OF PHYSICAL CHEMISTRY B

Article

pubs.acs.org/JPCB

Triaspartate: A Model System for Conformationally Flexible DDD Motifs in Proteins

Laura Duitch,[†] Siobhan Toal,[†] Thomas J. Measey,[‡] and Reinhard Schweitzer-Stenner*[,†]

[†]Department of Chemistry, Drexel University, 3141 Chestnut Street, Philadelphia, Pennsylvania 19104, United States

[‡]Department of Chemistry, University of Pennsylvania, Philadelphia, Pennsylvania 19104, United States

ABSTRACT: Understanding the interactions that govern turn formation in the unfolded state of proteins is necessary for a complete picture of the role that these turns play in both normal protein folding and functionally relevant yet disordered linear motifs. It is still unclear, however, whether short peptides can adopt stable turn structures in aqueous environments in the absence of any nonlocal interactions. To explore the effect that nearest-neighbor interactions and the local peptide environment have on the turn-forming capability of individual amino acid residues in short peptides, we combined vibrational (IR, Raman, and VCD), UV-CD, and ^{1}H NMR spectroscopies in order to probe the conformational ensemble of the central aspartic acid residue of the triaspartate peptide (DDD). The study was motivated by the recently discovered turn propensities of aspartic acid in GDG (Hagarman; et al. *Chem.—Eur. J.* **2011**, *17*, 6789). We investigated the DDD peptide under both acidic and neutral conditions in order to elucidate the effect that side-chain protonation has on the conformational propensity of the central aspartic acid residue. Amide I′ profiles were analyzed in terms of two-dimensional Gaussian distributions representing conformational subdistributions in Ramachandran space. Interestingly, our results show that while the protonated form of the DDD peptide samples various turn-like conformations similar to GDG, deprotonation of the peptide eliminates this propensity for turns, causing the fully ionized peptide to exclusively sample pPII and β-strand-like structures. To further explore the factors stabilizing these more extended conformations in fully ionized DDD, we analyzed the temperature dependence of both the UV-CD spectrum and the $^{3}J(H^{N},H^{\alpha})$ coupling constants of the two amide protons (N- and C-terminal) in terms of a simple two-state (pPII−β) thermodynamic model. Thus, we were able to obtain the enthalpic and entropic differences between the pPII and β-strand conformations of the central and C-terminal residue. For the central residue, we obtained $\Delta H_3 = -12.0$ kJ/mol and $\Delta S_3 = -73.8$ J/mol·K, resulting in a much larger room-temperature Gibbs free energy of 10.0 kJ/mol, which effectively locks the C-terminal in a β-like conformation. A comparison of the temperature dependence of the chemical shifts reveals that there is indeed some type of protection of the amide protons from solvent in ionized DDD. This finding and several other lines of evidence suggest that both conformations of ionized DDD are stabilized by hydrogen bonding between the carboxylate groups of the central and C-terminal residue and the respective amide protons. These hydrogen bonds can be expected to be eliminated by side-chain protonation and substituted by hydrogen bonds between the N-terminal amide proton and the C-terminal carbonyl group as well as between the central aspartate side chain and the N-terminal amide proton. Hence, our results are indicative of a pH-induced switch in hydrogen-bonding patterns of aspartic acid motifs.

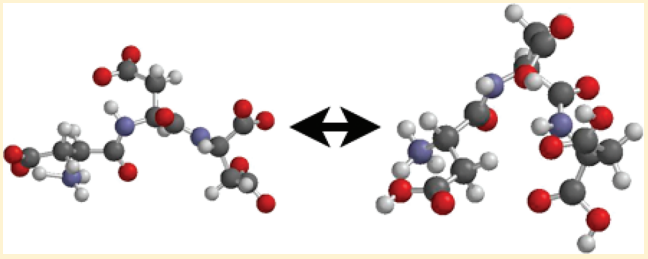

INTRODUCTION

The unfolded state of proteins and peptides has attracted considerable attention over the last 20 years. One of the reasons is the discovery of so-called intrinsically disordered proteins, which perform important biological functions even though they do not exhibit a well-defined tertiary or secondary structure.[1−6] The second reason is that evidence has been accumulated in support of the notion that unfolded proteins and peptides can exhibit local order, which is at variance with expectations from the classical random coil model.[7−16] Basically, two types of local order are discussed in the literature. Type 1 encompasses different types of turns,[8,9,16−18] whereas type 2 contains amino acid residues with an above-average propensity for polyproline II (pPII)-like conformations.[12,19−27] This paper focuses on type 1 structures in that it elucidates the propensity of aspartic acid residue to populate turn-like conformations even in very short peptides.

The relevance of turn formation in the unfolded state of proteins has been emphasized in a series of papers by Dyson, Wright, and their associates. By means of NMR spectrosocopy they provided evidence for the role of turns in the initial phase of protein folding.[8−10] Turn-like conformations have also been detected in the denatured state of proteins. Mukrasch et al. showed that an intrinsically disordered tau protein contains short aspartic acid-rich segments with a preference for type I β conformations.[28] Bystroff and Baker, by relating the local

Received: December 16, 2011
Revised: February 17, 2012
Published: March 21, 2012

   dx.doi.org/10.1021/jp2121565 | *J. Phys. Chem. B* 2012, 116, 5160−5171

structure of proteins to specific sequences, found that PGD(N) and PD(N)G segments have a high propensity for β-turns, whereas DPxTG (x: exchangeable residue) forms a turn stabilized by side-chain (D,N)-amide hydrogen bonding.[29]

The question arises whether or not short peptide fragments can form partially stable turn structures in water without the support of nonlocal interactions (e.g., of β-sheets.) Several lines of evidence suggest that this is indeed possible for proline-containing segments, though results from different experiments are not unambiguous. Several PGx peptides were found to form β-turn-like structures in trifluoroethanol (TFE), whereas their UV-CD spectra indicate a random coil structure in water.[30] Raman and NMR data indicate that Ac-NPY-NHMe (with P in trans) but not Ac-YPN-HMe forms a type I β-turn in water.[31,32] Peptides with proline in a cis conformation form type VI β-like turns. All of these turns are in equilibrium with more extended structures due to the absence of nonlocal interactions. Dyson et al., who have investigated a huge number of peptide fragments by NMR spectroscopy, found that YPxDV favors β-turns if P is in a trans conformation.[9] For the respective cis conformation, only AYPYDV forms a turn (type VI). β-turns can also be formed by YQNPDGSQA, VPGK, and GPER.[12,33] Proline at the i + 1 position is not a necessary ingredient for turn formation, as documented by the turn-forming capabilities of, for example, DLKN, DLSN, and DLSK motifs in the unfolded tau protein,[28] the type VIII β-turn-forming peptide, GDNP,[34] the sampling of type I, II′, IV, and V′ β-type turns by peptides with the RGD motif,[35−38] and the involvement of hydrophobic residues in turn-forming motifs (i.e., LIAVP, IVF).[39] Turn propensities are often obtained from the comprehensive investigations of Chou and Fasman.[40] However, it is unclear whether propensities obtained from intact proteins reflect intrinsic turn-forming capabilities. A comparison of turn propensities obtained from energy minimization of dipeptides in vacuo and from 20 proteins showed a satisfactory agreement for only 26 out of 47 dipeptides.[41]

The above propensity studies suggest that polar residues play an important role in the formation of turns. This is particularly the case in so-called asx and ST turns, in which D, N, S, and T are positioned at the i or i + 1 position. These turns, which appear frequently in proteins, bear similarities with β-turns, but in contrast to classical turns, they are formed by hydrogen bonding between the polar side chains of the above polar residues and backbone amide groups.[42−45] The question arises whether they can be formed in aqueous solution. It is generally thought that this requires the presence of either P or aminoisobutyric acid (Aib) residues at the ith position or an insertion of a D-amino acid at the i + 2 position. Song et al. showed that the modification of the serine side chain to homoserine also promotes ST-like turns.[45] However, a recent study on selected GxG peptides in aqueous solution with x = S, T, C, N, and D by NMR and vibrational spectroscopy revealed a disproportional sampling of various β-turn-like conformations.[46] Additionally, (protonated) D and, to a lesser extent, N sample a conformation that is assignable to the upper border region of the upper-right quadrant of the Ramachandran plot. Similar conformations have been found in the aforementioned asx-turns.[44]

In the current paper, we further investigate the conformational propensities of aspartic acid by exploring the conformation ensemble of the central residue of DDD at acidic and neutral pH by vibrational, circular dichroism (CD), and ^{1}H NMR spectroscopy. This study serves several purposes. First, a comparison of DDD with acidic, fully protonated GDG and of different protonation states of DDD allows us to identify the influence of nearest neighbors on the conformational propensity of D. For GDG, we can reasonably well assume that the obtained ensemble of D reflects the intrinsic conformational propensity of protonated D in the unfolded state of peptides and proteins. Aspartic acid has a sterically more demanding side chain than glycine; it can be either polar (in the protonated state) or ionized (in the deprotonated state), and it has the capability to donate and accept hydrogen bonding. Earlier experiments have shown that the conformation of charged lysine is different in a polylysine then it is in alanine-based peptides, which indicates that electrostatic interactions between ionized neighbors can affect the conformational distributions of the involved amino acid residues.[47−49] This study is aimed at checking whether this is the case for DDD. Second, our study will shed some light on the structural properties of DxD motifs, which appear in so-called linear motifs, that is, conformationally disordered but functionally relevant segments of various proteins.[50,51] DSD and DDD segments, for example, are representatives of the DxD motif in the nucleotide-binding capacity of the Golgi glycosyltransferase GM2 synthase.[51] The DDD segment of this protein is thought to be located between the strands of the β-sheet structure, which should create a rather hydrophobic environment in which the side chains are likely protonated.[52] Thus, it is important to investigate the protonated as well as the deprotonated state of DDD. Third, the results of our study could be expected to shed some further light on the turn-forming capability of aspartic acid, which, in view of the abundance of D in turn-forming segments, is of general relevance.[40]

An earlier structural analysis of DDD at neutral pH has been reported by Eker et al.[47] The authors interpreted the amide I profiles of the peptide's IR, isotropic Raman, anisotropic Raman, and vibrational circular dichroism (VCD) spectra in terms of a single, representative structure, which they interpreted as distorted pPII. In the current study, a more detailed analysis reveals the conformational distributions that DDD adopts at both neutral and acidic pH.

MATERIALS AND METHODS

Materials. L-Aspartic acid-L-aspartic acid-L-aspartic acid (DDD) was obtained from Bachem (Torrance, CA). L-glycyl-L-aspartic acid-L-glycine (GDG) was custom synthesized by Genscript corp. (Piscataway, NJ) at >98% purity and subsequently dialyzed against HCl to remove residual trifluoroactic acid (TFA), which absorbs in the amide I′ region.

Vibrational and UV-CD spectra of DDD and were measured in both acidic (pD = 2.1), and neutral (pD = 7.8) D_2O at peptide concentrations of 0.15 M and 5 mM for vibrational and UV-CD experiments, respectively. Peptide solutions were adjusted to the desired pD value by titration with DCl and NaOD. The pD values were determined via the method of Glasoe and Long[53] using an Accumet microsize glass electrode and pH meter (Fischer Scientific). For ^{1}H NMR measurements of DDD, the peptide was dissolved at a concentration of 0.2 M in a solution of 90% H_2O/10% D_2O (1% TMS), at two pH values, acidic (pH = 2.0) and a mildly acidic solution of pH = 5.1. The mildly acidic choice of pH here was necessary to ensure that the aspartic acid side chains were ionized and yet the amide signal for the backbone was clearly resolved.

dx.doi.org/10.1021/jp2121565 | J. Phys. Chem. B 2012, 116, 5160−5171

Vibrational and CD Spectroscopy. The experimental setup for polarized Raman, IR, VCD, and UV-CD experiments have been previously described in detail.[60] UV-CD spectra were measured between 190 and 300 nm at different temperatures between 10 and 80 °C with 10 °C increments for acidic DDD and 5 °C increments for neutral DDD using a Jasco J-810 spectrometer. The spectra were collected as ellipticity as a function of wavelength and converted to $\Delta\varepsilon$ (M^{-1} cm^{-1} res^{-1}), where the number of residues equals 2 for DDD. The amide I region of IR and isotropic and anisotropic Raman spectra were self-consistently decomposed into individual Voigtian bands by using the program MULTIFIT.[54] Self-consistency means that related bands in Raman and IR spectra had the same wavenumbers and bandwidths. Subsequently, intense bands assignable to the C-terminal CO stretching vibration (fully protonated DDD) and the antisymmetric COO stretching vibration (fully ionized DDD) were subtracted from the spectra in order to isolate the respective amide I band profiles.

^{1}H NMR Spectroscopy. The temperature dependence of ^{1}H NMR amide proton signals for DDD was measured on a 500 MHz Varian FT-NMR instrument equipped with a 5 mm HCN triple resonance probe. For acidic DDD, spectra were collected from 25 to 65 °C with 10 °C intervals. Spectra for DDD in the mildly acidic and ionized form (pH = 5.1) were collected from 25 to 45° with 5 °C intervals. The sample temperature was controlled using a Varian VT controller, and the sample was allowed to equilibrate at each temperature for 100 s after reaching the target temperature. Mestre-C (Mestrelab Research) was used to process all raw spectra. Deconvolution and fitting of the amide proton signals with Lorenztian band profiles was carried out using MULTIFIT.[54] The temperature dependence of all $^3J(H^N,H^\alpha)$ coupling constants were determined by first converting the chemical shift values of the two peaks of doublets into frequencies (Hz). Second, we plotted these frequency values as a function of temperature. Third, we subjected these plots to linear regression analysis. Finally, we subtracted values of these two fits that corresponded to our experimentally obtained temperatures to yield the respective $^3J(H^N,H^\alpha)$ values. Details of this strategy are described by Toal et al.[55]

THEORETICAL BACKGROUND

The theory used for the data analysis has been described in detail in earlier publications.[56−58] Here, we briefly reiterate the aspects that are essential for an understanding of this paper.

To construct a model for the conformational ensemble sampled by the central residue of DDD, we subdivided the Ramachandran space into mesostates, each of which is represented by a two-dimensional Gaussian distribution. These mesostates, which are also visualized in Figure 1, are defined as follows: (1) antiparallel β-strand (aβ) ($-130° > \varphi_{max,3} \geq -180°$; $180° > \psi_{max,3} \geq 100°$), (2) the transition region between the antiparallel β-strand and pPII (aβt) ($-90° > \varphi_{max,3} \geq -130°$; $180° > \psi_{max,3} \geq 140°$), (3) pPII ($-60° > \varphi_{max,1} \geq -90°$; $180° \geq \psi_{max,1} > 100°$), (4) parallel β-strand (pβ) ($-100° > \varphi_{max,2} \geq -130°$; $140° > \psi_{max,2} \geq 100°$), (5) dihedral angles of the $i + 1$ residue in type I β-turns (these are the dihedral angles adopted by residues in right-handed α-helices) ($-50° > \varphi_{max,5} > -80°$; $-20° > \psi_{max,5} > -40°$), (6) dihedral angles of the $i + 2$ residue in type I and II′ β-turns as well as both corner residues in type IV β-turns (these are the dihedral angles adopted by residues considered in the extended right-handed α-helix distribution) ($-50° > \varphi_{max,7} > -110°$; $20° > \psi_{max,7} > -20°$), and (7) dihedral angles found in asx-turns ($80° > \varphi_{max} > 50°$; $170° > \psi_{max} > 50°$).

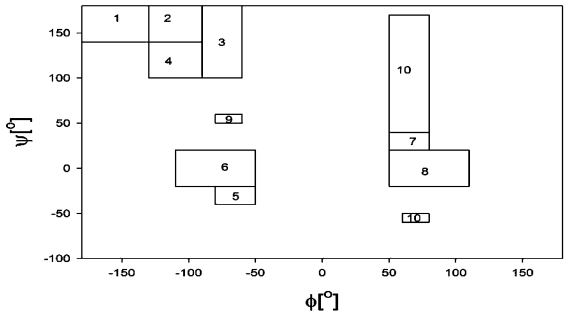

Figure 1. Representative Ramachandran representation of the mesostates considered for simulating the amide I′ band profile and NMR coupling constants. These states are described in detail in the Theoretical Background section.

The conformational distribution of DDD was obtained by measuring and analyzing the amide I′ band profile of its IR, isotropic Raman, anisotropic Raman, and VCD spectra. Our analysis of these profiles considers excitonic coupling between the two local amide I′ modes in the tripeptides, which increases the splitting between them and redistributes IR and Raman intensities.[57] Excitonic coupling itself and the degree of redistribution of the intensities depends on the dihedral angles of the central residue located between the two interacting oscillators. The underlying theory as well as the formalism and the empirical parameters used for the simulation of amide I′ band profiles have been described in detail in numerous papers, to which the interested reader is herewith referred.[57−60]

We constrained our analysis of the amide I profiles by the $^3J(H^N,H^\alpha)$ constant of the N-terminal amide proton. It is related to the dihedral angle ϕ by the Karplus equation[61]

$$^3J = A\cos^2(\phi - \pi/3) + B\cos(\phi - \pi/3) + C \quad (1)$$

where the newest empirical constants A, B, and C are reported by Graf et al.[62]

The conformational manifold sampled by the central residue of the investigated DDD peptides is described in terms of an ensemble of mesostates, using superimposed two-dimensional Gaussian distribution functions[57]

$$f_j = \left(\frac{\chi_j}{2\pi\sqrt{|\hat{V}_j|}}\right) e^{-0.5\cdot(\vec{\rho}-\vec{\rho}_j^{\,0})^T\hat{V}_j^{-1}(\vec{\rho}-\vec{\rho}_j^{\,0})} \quad (2a)$$

where

$$\rho = \begin{pmatrix}\phi\\ \psi\end{pmatrix} \quad (2b)$$

and

$$\hat{V} = \begin{pmatrix}\sigma_{\phi,j} & \sigma_{\phi\psi,j}\\ \sigma_{\phi\psi,j} & \sigma_{\psi,j}\end{pmatrix} \quad (2c)$$

The vector $\vec{\rho}$ points to the position of the maximum of the jth distribution in the (ϕ,ψ) space, and χ_j is its statistical weight, which we use as a quantitative measure of a residue's intrinsic propensity for the conformation j. The diagonal elements of the matrix $\hat{V}_j$ are the half-halfwidths of the jth distribution along the coordinates ϕ and ψ, and the off-diagonal elements reflect correlations between variations along the two coordinates. If $\hat{V}_j$

dx.doi.org/10.1021/jp2121565 | J. Phys. Chem. B 2012, 116, 5160−5171

is diagonal, the ϕ,ψ projection of the distribution is an ellipse with its main axes parallel to the ϕ and ψ axes.

The expectation value of any observable x (spectral intensities, rotational strengths, J coupling constants) can be written as

$$\langle x \rangle = \frac{\int_{-\pi}^{\pi}\int_{-\pi}^{\pi} x \cdot f(\phi, \psi)\, d\phi\, d\psi}{Z} \quad (3)$$

where Z denotes the canonical partition sum.

For our analysis, we calculated amide I band profiles and J coupling constants for each of the considered conformations and subsequently used eqs 2−3 to obtain the corresponding profiles and coupling constant for the considered conformational ensembles.

RESULTS AND DISCUSSION

In order to facilitate the understanding of this section, we find it beneficial to outline the investigated DDD peptide, as shown in Figure 2. DDD contains three residues (i = 1, 2, and 3) with

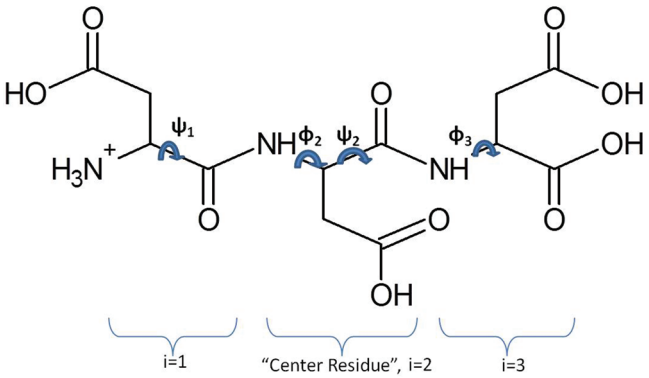

Figure 2. Fully protonated DDD with N-terminal and C-terminal amide groups outlined for reference. For HNMR analysis, it is necessary to consider two amide protons resulting in two $^3J(H^N,H^R)$ values associated with two different φ-values (φ_2 and φ_3). ϕ_N is associated with the central aspartic acid, as outlined in the figure.

two amide protons. The latter give rise to two doublets in the ^{1}H NMR spectrum, from which the respective $^3J(H^N,H^\alpha)$ coupling constants can be inferred. These coupling constants are related to the ϕ angles of the central (i = 2) and the C-terminal residue (i = 3) according to the Karplus equation.[61] The N-terminal residue (i = 1) itself is not directly associated with an exchangeable amide proton. When discussing our ^{1}H NMR data, we follow Oh et al.[63] by referring to the $^3J(H^N,H^\alpha)$ coupling constant associated with the central residue's ϕ angle as the "N-terminal" ($^3J_N(H^N,H^\alpha)$) because it belongs to the N-terminal peptide group. The second $^3J(H^N,H^\alpha)$ constant, which is a function of the ϕ angle of the third (i = 3) residue, is consequently termed the "C-terminal" ($^3J_C(H^N,H^\alpha)$). With our vibrational spectroscopic techniques, however, we are exploiting the excitonic coupling between amide I′ oscillators, which solely depends on the conformational distribution of the central residue (Figure 2).

This following section is organized as follows. We first introduce and qualitatively discuss the UV CD spectra and ^{1}H NMR (chemical shifts and $^3J(H^N, H^\alpha)$) constants of fully protonated and fully ionized DDD (denoted as DDD^p and DDD^i in the following). In a second step, we describe the results of a structural analysis of these two protonation states of the peptide based on amide I′ band profiles and $^3J(H^N, H^\alpha)$ constants. In the last section, we analyze the temperature dependence of the UV-CD spectra and the $^3J(H^N,H^\alpha)$ constants of fully ionized DDD in terms of a two-state thermodynamic model

UV-CD and ^{1}H NMR Spectroscopy. We measured the UV-CD spectra of DDD^p at pD 1.7 as a function of temperature between 5 and 90 °C, which are depicted in Figure 3. A

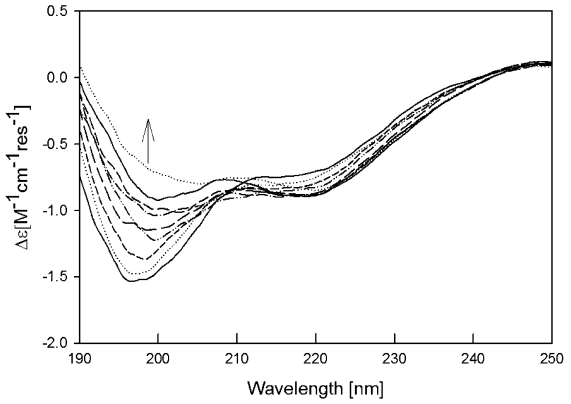

Figure 3. UV-CD spectrum of fully protonated DDD measured at pD = 1.7 as a function of temperature between 10 and 90 °C in increments of 10 °C. The arrow indicates increasing temperature.

comparison of these UV-CD spectra with earlier recorded spectra of cationic trialanine (AAA) is made in Figure 4 by plotting the spectra of both peptides on the same scale. Using AAA as a reference system is beneficial because among all amino acid residues, alanine deviates mostly from a random coil behavior in that it exhibits the highest pPII propensity with

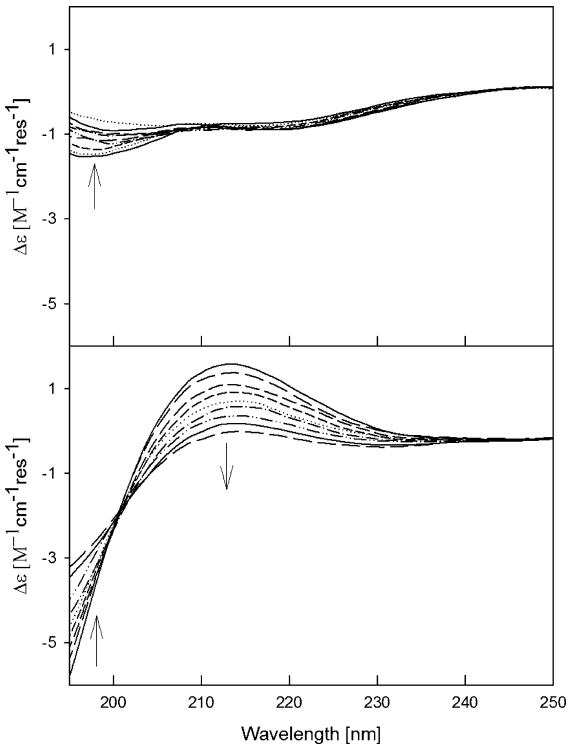

Figure 4. Comparison of the temperature-dependent UV-CD spectrum of acidic DDD (upper panel) and acidic AAA (lower panel).

dx.doi.org/10.1021/jp2121565 | J. Phys. Chem. B 2012, 116, 5160−5171

pPII fractions between 0.8 and 0.95 at room temperature.[55,57,62,64] If flanked by glycine or alanine residues, alanine shows a two-state behavior, that is, an equilibrium between pPII and β-strand conformations, where the latter become more stabilized with increasing temperature.[55,64,65] The respective spectra of DDD^{P} and AAA are both qualitatively and quantitatively different. The negative maximum below 200 nm is much more pronounced for AAA than that for DDD^{P}. All spectra of the former share an isodichroic point at 200 nm, which is indicative of the aforementioned two-state behavior. While the DDD^{P} spectra recorded between 5 and ~60 °C exhibit an isodichroic point at 210 nm, it is not shared by the spectra measured at higher temperatures. This indicates a departure from a two-state behavior for DDD^{P} at high temperatures. Finally, the CD spectrum of AAA exhibits a weak positive maximum at 215 nm, which is diagnostic of pPII dominating the conformational distribution.[63,64,66−70] The spectra of DDD^{P}, however, show a shallow but clearly discernible negative maximum at this wavelength, which was also observed by Hagarman et al. for GDG, which was found in their analysis to form turn-like conformations in aqueous solution.[46] Apparently, DDD^{P} populates more than two states. The validity of this conclusion becomes even more obvious if one plots the dichroism measured at 196 and 216 nm as a function of temperature (Figure 5). The former exhibits a

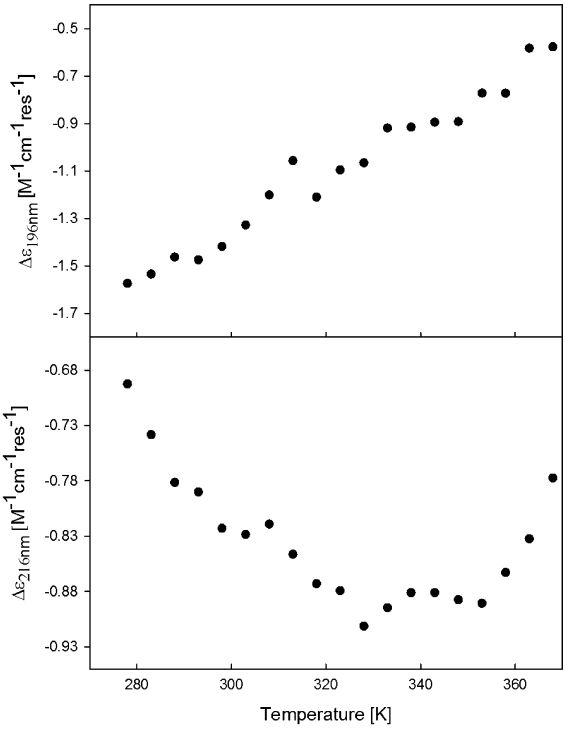

Figure 5. $\Delta\varepsilon_{196\,nm}$ (upper panel) and $\Delta\varepsilon_{216\,nm}$ (lower panel) of DDD^{P} plotted as a function of temperature.

nearly linear behavior, which is typical for a redistribution of sampling between two distinct conformations. However, the 216 nm data clearly show a biphasic behavior. The negative values first increase with temperature and reach a plateau at ~50 °C. Above 70°, the $\Delta\varepsilon$ value suddenly increases. This coincides with the loss of the isodichroic point.

We also measured the UV-CD spectrum of DDD^{i} (at pH = 5) as a function of temperature. The spectra are shown in Figure 6. They are quite distinct from the spectra of DDD^{P} in that they show a nearly symmetric couplet with a very

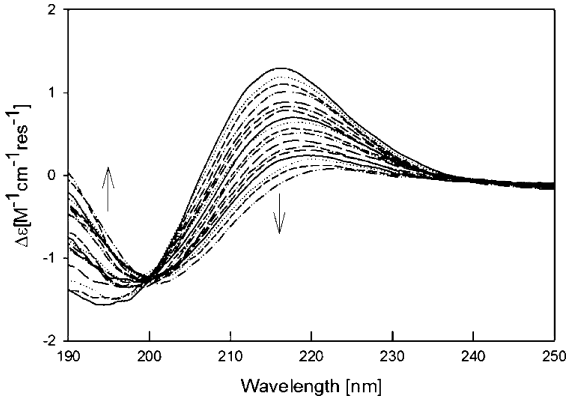

Figure 6. UV-CD spectrum of DDD^{i} measured at pD = 7 as a function of temperature between 10 and 90 °C in increments of 5 °C.

pronounced positive maximum and a clearly discernible isodichroic point at 200 nm. Similar spectra have been reported before by Eker et al.[70] The temperature dependence of $\Delta\varepsilon$ recorded at 216 nm is shown in Figure 7. It shows the nearly

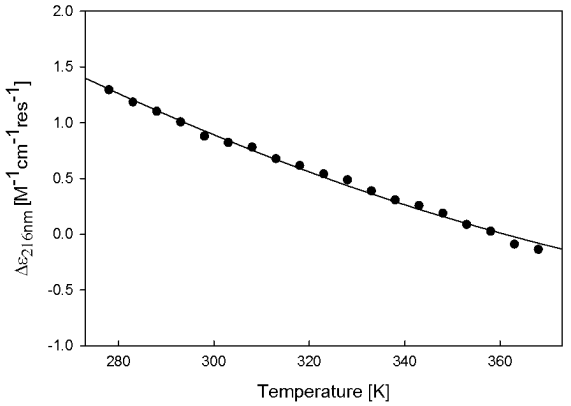

Figure 7. $\Delta\varepsilon_{216}$ of DDD^{i} measured at 216 nm plotted as a function of temperature. The solid line results from the fitting process described in the text.

linear behavior typical for a population redistribution between two states. The difference between the symmetric couplets of DDD^{i} and the typical pPII-indicating negatively biased couplet of AAA might in part reflect contributions of charge-transfer transitions between n-orbitals of the four carboxylate groups and the π^*-LUMO of the peptide groups.[71]

The $^{3}J(H^{N},H^{\alpha})$ coupling constants of both amide protons obtained from ^{1}H NMR spectra measured at room temperature are listed in Table 1 for both the fully protonated and the fully

Table 1. Room-Temperature $^{3}J(H^{N},H^{\alpha})$ Coupling Constants for the N- and C-Terminal Residues of Fully Protonated and Fully Ionized DDD Obtained by the Procedure of Toal et al.[55]

	N-terminal $^{3}J(H^{N},H^{\alpha})$ [Hz]	C-terminal $^{3}J(H^{N},H^{\alpha})$ [Hz]
protonated DDD	7.46	8.04
ionized DDD	7.22	7.62

dx.doi.org/10.1021/jp2121565 | J. Phys. Chem. B 2012, 116, 5160−5171

ionized state of the peptide. It should be reiterated that the NMR spectra of DDD[i] had to be recorded at mildly acidic conditions (pH = 5) to ensure that the amide proton signals were still measurable. At both pH values investigated, the $^3J(H^N,H^\alpha)$ values of the N-terminal proton on the central residue are lower than the respective C-terminal values, which indicates differences between the conformational distributions. A similar discrepancy was obtained for AAA.[72] Interestingly, the two N-terminal values of DDD for both pH values studied are similar (7.22 and 7.46 Hz for the ionized and protonated state, respectively) and close to the value reported for GDG (7.5 Hz) at acidic pH.[46] Thus, on the basis solely of these NMR data, one would conclude that the conformational distributions of GDG and DDD at acidic pH and of DDD at neutral pH are all very similar. As we will see below, this conclusion would be incorrect. For the C-terminal residues, the ionized state shows a somewhat lower $^3J(H^N, H^\alpha)$ coupling (7.62 Hz) constant than the protonated state (8.04 Hz).

Vibrational Spectroscopy. Figures 8 and 9 show the IR, isotropic Raman, anisotropic Raman, and VCD band profiles of the amide I′ mode of fully protonated and fully ionized DDD in D_2O. The profiles were isolated by the procedure described in the Materials and Methods section. The amide I′ profiles of fully protonated DDD resemble to some extent an earlier observation for GDG, in that the IR and both Raman profiles are more intense at the position of the high-wavenumber band that is assignable to the N-terminal amide I′ mode.[46] This is unusual because the corresponding IR band profiles of other peptides are normally more intense at the low-wavenumber band, which is attributed to the C-terminal amide I′ mode.[73] This produces a noncoincidence between the first moments of isotropic Raman and IR band profiles, which is indicative of the dominance of extended structures like pPII and β-strand.[56,74] The absence of this noncoincidence in the spectra of fully protonated DDD suggests more compact turn-like conformations, which have indeed been identified for fully protonated GDG.[42] We used the distribution function recently obtained for this peptide as a starting point for our simulations of the amide I′ band profiles in Figure 8. A modification was necessary to particularly account for the practically absent VCD signal. The final result of our simulation is visualized by solid lines in Figure 8, which show excellent agreement with experimental data for DDD[p] (dotted lines). In addition, the simulation yields a $^3J_N(H^N,H^\alpha)$ coupling of 7.47 Hz, in agreement with the experimentally obtained value of 7.46 Hz. The coordinates of the two-dimensional Gaussian distributions associated with the involved conformations are listed in Table 2.

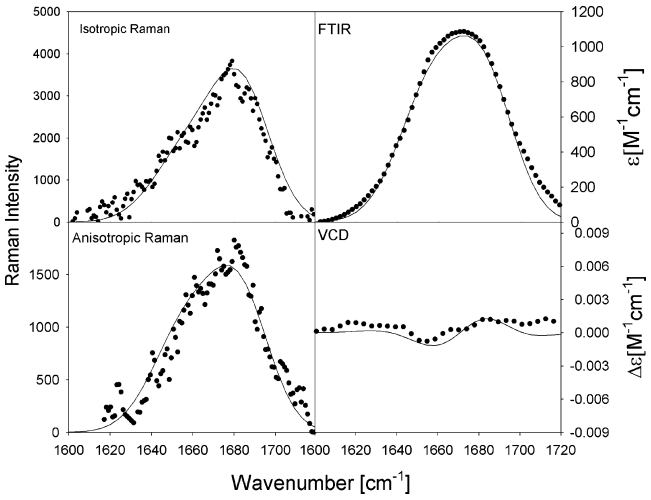

Figure 8. Amide I′ band profiles of DDD[p] measured at pD = 1.7. The solid lines result from a simulation described in the text.

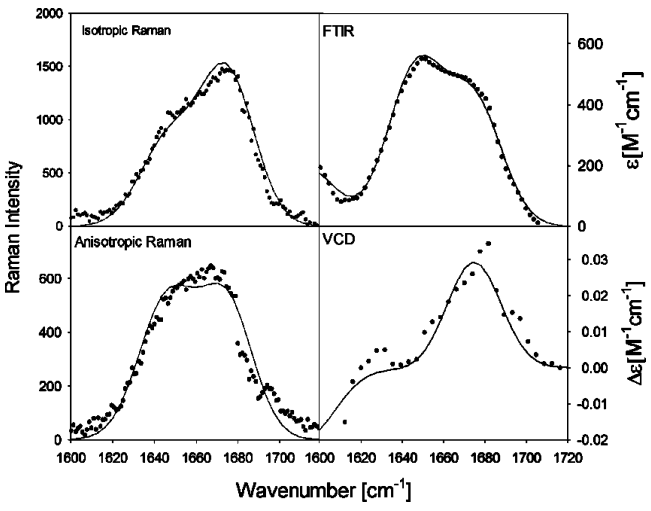

Figure 9. Amide I′ band profiles of DDD[i] measured at pD = 7. The solid lines result from a simulation described in the text.

Table 2. List of Conformations of DDD and Their Respective Mole Fractions Inferred from Amide I′ Band Profiles and the Respective N-Terminal $^3J(H^N,H^\alpha)$ Coupling Constant[a]

conformation	protonated DDD	ionized DDD
pPII [−74°, 135°, 3]		0.59
aβt {[−126°, 170°, 2][b] and [−100°, 140°, 2][c]}	0.32	0.41
i + 1 type I/type III β-turn [−60°, −30°, 5]	0.31	
aβ{ [−130°, 170°, 1] and [−130, 135, 1]	0.17	
upper right quadrant [55°, 170°, 10]	0.05	
i + 2 type I/II turn [−70°, 0°, 6]	0.05	

[a]The numbers in parentheses are the ϕ and ψ values of the respective center of the two-dimensional Gaussian distribution and the number of the respective mesostate. The half-halfwidth of the distribution was 10°, with the exception of pPII, for which σ_ϕ = 20°. The off-diagonal elements of the covariance matrices are 0. [b]For protonated DDD. [c]For ionized DDD.

Compared with the distribution found for acidic GDG, the current results for DDD[p] indicate a lesser sampling of mesostate 7, which Hagarman et al. associated with asx-turns.[46] The population is nearly equally distributed over two extended conformations covering mesostates 2, 3, and 4, and right-handed helix-like conformations, which also appear in type I and III β-turns. A small fraction resides in mesostate 6, which contains conformations found at the i + 2 positions of type I and II′ β-turns. As for GDG, we did not identify a significant population of pPII conformations. Altogether, more than 40% of the peptides in the sample are in some type of turn conformation. This is slightly lower than the value for GDG, which lies above 50%. Thus, the result indicates some modest modification of the conformational distribution of D by the protonated aspartic acid side chains.

dx.doi.org/10.1021/jp2121565 | J. Phys. Chem. B 2012, 116, 5160−5171

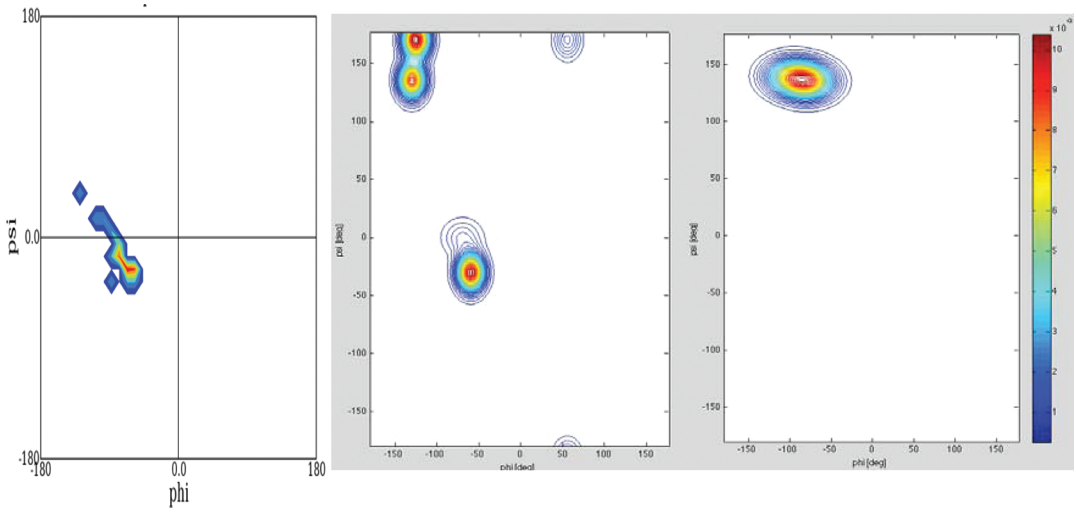

Figure 10. (Middle) Conformational distribution of the central residue in DDD^{P} as obtained from the combined analysis of amide I profiles and the $^{3}J(H^{N},H^{\alpha})$. (Right) Conformational distribution of the central residue in DDD^{i} as obtained from the combined analysis of amide I profiles and the $^{3}J(H^{N},H^{\alpha})$. (Left) Conformational distribution of aspartic acid in DDD segments of truncated coil libraries. Truncated means that all residues residing in helices and sheets have been omitted. Obtained from ref 76.

The amide I′ band profiles of the fully ionized peptide are shown in Figure 9, together with the results of the respective simulations. The latter had to reproduce the positive Cotton band in the VCD spectrum, which is quite unusual for VCD spectra of peptides but which reproduces earlier experiments by Eker et al.[47] To account for this signal, an intrinsic magnetic transition dipole moment of -1.2×10^{-23} esu cm had to be assumed for the N-terminal residue. In contrast to what we observed for DDD^{P}, the IR and isotropic Raman profiles show the noncoincidence that is typical for extended structures. However, the low-wavenumber component of the isotropic band profile carries much more intensity than, for example, the corresponding band in the spectrum of AAA.[59] This indicates a much weaker excitonic coupling between the two local amide I modes in DDD^{P}. Our analysis did not yield an unambiguous result in that simulations of similar quality could be found by using different mixtures of pPII and β-strand conformers depending on which mesostates had been chosen for the latter. The best among barely distinguishable fits yielded a mixture of pPII and aβt in mesostates 3 and 2, respectively. The pPII distribution overlaps with the region sampled by the first amino acid residues in type II β-turns. However, our assessment became somewhat more accurate when we tried to use the results of this simulation to impose constraints on our analysis of the temperature dependence of the N-terminal $^{3}J(H^{N},H^{\alpha})$ constants. As described in the next section, only a small range of values for pPII and aβt allowed satisfactory fitting of the thermodynamic data derived from NMR. Table 2 lists the distribution parameters that eventually emerged from this analysis.

Our results from the vibrational analysis clearly show that deprotonation of the aspartate neighbors eliminates the propensity of the central D for turns. That is per se an important example of the relevance of nearest-neighbor interaction and side-chain charges in DDD motifs. It is interesting to compare our results with the coil library distribution obtained by Sosnick and co-workers.[75,76] We selected the distribution of the truncated library from which helical and strand conformations have been omitted. As shown in Figure 10, the single cluster in the Ramachandran plot of DDD occurs in the region that can be attributed to mesostate 6. These conformers can be found at the $i + 2$ position of type I and II β-turns and are close to the trough of right-handed helical conformers. Generally, this coil library distribution is clearly different from the two distributions that we obtained for DDD^{P} and DDD^{i}, which are also shown in Figure 10 for comparison. However, our results indicate some overlap between the coil library distribution and that of the protonated peptide in that both indicate sampling of the adjacent mesostates 5 and 6. We suspect that the difference between the coil library and tripeptide distributions reflects different degrees of solvation, which could be expected to favor extended structures. This comparison shows that coil library distributions do not necessarily represent the conformational propensities of amino acid residues in aqueous solution.

Thermodynamic Analysis. We determined the temperature dependence of the $^{3}J(H^{N},H^{\alpha})$ coupling constants of the two amide protons from the regression analysis of the temperature dependences of the individual chemical shifts of the split amide proton doublets as described in the Materials and Methods section. For DDD^{P}, the temperature dependences of the frequency positions of the N- and C-terminal amide proton doublets are depicted in Figure 11. From a linear fit to these data, we obtained the temperature dependence of $^{3}J_{N}(H^{N},H^{\alpha})$ and $J_{C}(H^{N},H^{\alpha})$, as shown in the inset of Figure 11. The C-terminal $^{3}J(H^{N},H^{\alpha})$ constant is nearly temperature-independent, whereas the corresponding constant of the N-terminal slightly decreases with increasing temperature. This very surprising and unusual result shows that the temperature dependence of the CD spectra predominantly reflects changes along the ψ angle of both the central N-terminal and C-terminal D residue. This is very much in contrast to what one normally observes for tripeptides where conformational redistributions occur predominantly along the ϕ angle, thus causing a comparable temperature dependence of UV-CD spectra and the $^{3}J(H^{N},H^{\alpha})$ constant.[55,65]

The UV-CD and NMR data of DDD^{i} allow for a quantitative thermodynamic analysis of the conformationally sensitive parameters $^{3}J(H^{N},H^{\alpha})$ and $\Delta\varepsilon_{216\ nm}$ (i.e., the dichroism value of the positive maximum for the room-temperature UV-CD

dx.doi.org/10.1021/jp2121565 | J. Phys. Chem. B 2012, 116, 5160−5171

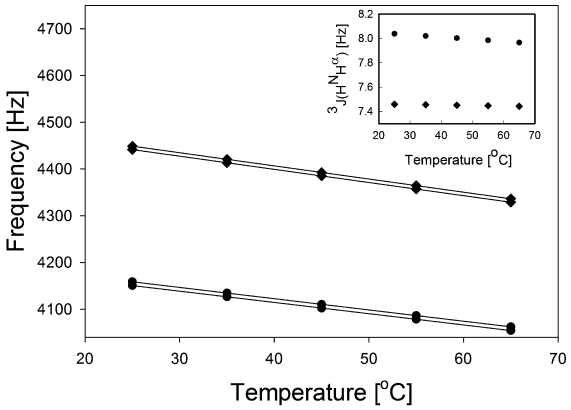

Figure 11. Chemical shift of the two amide proton bands of the N-terminal (●) and C-terminal (♦) peptide groups for fully protonated DDD, plotted as a function of temperature. The solid lines result from linear least-squares fits to the data. The results from these fits were used to calculate the temperature dependence of the respective $^3J(H^N,H^\alpha)$ coupling constants as a function of temperature. The result of this procedure is visualized by the points in the inset, which represent the $^3J(H^N,H^\alpha)$ values for the temperatures at which the chemical shifts have been measured.

spectrum). The temperature dependence of the two $^3J(H^N,H^\alpha)$ parameters is shown in Figure 12. The existence of an

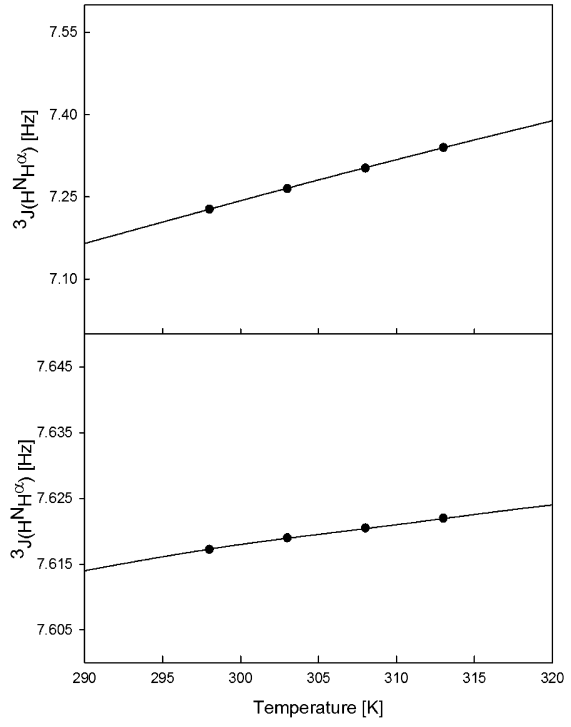

Figure 12. $^3J(H^N,H^\alpha)$ [Hz] of the N-terminal (upper panel) and C-terminal (lower panel) plotted as a function of temperature from 298 to 333 K for DDD^i. The solid line is a result of the two-state thermodynamic model fitting procedure described in the text.

isodichroic point in the UV-CD temperature dependence (Figure 6) indicates that the neutral form of the peptide predominantly samples two different conformational states, and hence, a simple two-state pPII ↔ β model can be applied in this case. This notion is consistent with the conformational ensemble obtained for DDD^i through vibrational analysis. Although the temperature dependence of the UV-CD spectrum is not as pronounced for DDD^i as it is for AAA (Figures 6 and 4, respectively), it is still clearly indicative of a conformational shift from pPII to a more extended β-strand-like conformation at higher temperatures. The fact that DDD shows a more symmetric couplet than the usual pPII-indicating spectra (e.g., that of AAA) is most likely attributable to contributions from n → π^* transitions between carboxylate groups and peptide linkages.[71] The uncertainty about contributions from these charge-transfer transitions does not exclude a two-state analysis. Following the protocol of Toal et al.,[55] we employed a global fitting procedure to simultaneously analyze the temperature-dependent dichroism ($\Delta\varepsilon_{216}$) (Figure 6) with a two-state model for the entire peptide and temperature-dependent $^3J(H^N,H^\alpha)$ values (Figure 12) with a two-state model for individual residues. In this analysis, the experimentally measured values of $^3J(H^N,H^\alpha)$ and $\Delta\varepsilon_{216\ nm}$ can be expressed in terms of mole-fraction-weighted contributions from each conformation, which in turn can be expressed as a function of temperature by the use of Boltzmann factors. For the site-specific $^3J(H^N,H^\alpha)$ constants measured as a function of temperature, this yields

$$J_i(T) = \frac{J_{\mathrm{pPII},i} + J_{\beta,i}e^{-\Delta G_i/RT}}{1 + e^{-\Delta G_i/RT}} \tag{4}$$

where $\Delta G_i = G_{\beta,i} - G_{\mathrm{pPII},i}$ denotes the Gibbs energy difference between pPII and the β-strand probed by the ith amide proton (i = 1 for the N-terminal, and i = 2 for the C-terminal), and $J_{\mathrm{pPII},i}$ and $J_{\beta,i}$ are the respective J coupling constants.

In order to fit $\Delta\varepsilon_{216}(T)$, we would normally use the thermodynamic parameters obtained from our fits to the N- and C-terminal $^3J(H^N,H^\alpha)(T)$ to calculate an effective Gibbs free energy and equilibrium constant.[55,65] Because experimental dichroism values obtained from UV-CD reflect two net populations of pPII and β, a slight modification of the expression for $\Delta\varepsilon$ was made to explicitly account for the mole fractions of all peptide conformations, that is, $\chi_{\mathrm{pPII-pPII}}$, $\chi_{\beta-\beta}$ $\chi_{\mathrm{pPII}-\beta}$, and $\chi_{\beta-\mathrm{pPII}}$. Assuming that corresponding $\Delta\varepsilon$ values for both residues are identical, one can directly write the $\Delta\varepsilon_{216}(T)$ as a superposition of contributions from all of these conformations

$$\begin{aligned}\Delta\varepsilon(T) = {} & (2\cdot\chi_{\mathrm{pPII-pPII}} + \chi_{\mathrm{pPII}-\beta} + \chi_{\beta-\mathrm{pPII}}) + \Delta\varepsilon_{\mathrm{pPII}} \\ & + (2\cdot\chi_{\beta-\beta} + \chi_{\mathrm{pPII}-\beta} + \chi_{\beta-\mathrm{pPII}})\Delta\varepsilon_\beta\end{aligned} \tag{5}$$

where $\Delta\varepsilon_{\mathrm{pPII}}$ and $\Delta\varepsilon_\beta$ are the dichroism values of residues in pPII and β at 216 nm. The factor 2 reflects the fact that two residues contribute to $\Delta\varepsilon_{\mathrm{pPII}}$ and $\Delta\varepsilon_\beta$, if both residues adopt pPII and β-strand conformations, respectively. For practical reasons, the intrinsic ellipticities $\Delta\varepsilon_{\mathrm{pPII}}$ and $\Delta\varepsilon_\beta$ are here expressed in units of M^{-1} cm^{-1}. The mole fractions in eq 5 can be expressed in terms of Boltzmann factors, which finally yields

$$\begin{aligned}\Delta\varepsilon_{216}(T) = {} & [\Delta\varepsilon_{\mathrm{pPII}}(2 + e^{-\Delta G_2/RT} + e^{-\Delta G_3/RT}) \\ & + \Delta\varepsilon_\beta(e^{-\Delta G_2/RT} + e^{-\Delta G_3/RT} \\ & + e^{-(\Delta G_2+\Delta G_3)/RT})]/[1 + e^{-\Delta G_2/RT} \\ & + e^{-\Delta G_3/RT} + e^{-(\Delta G_2+\Delta G_3)/RT}]\end{aligned} \tag{6}$$

where $\Delta G_i = G_{\beta,i} - G_{\mathrm{pPII},i}$ is the Gibbs energy difference between the two considered conformations of residue i (where

dx.doi.org/10.1021/jp2121565 | J. Phys. Chem. B 2012, 116, 5160–5171

Table 3. (a) Spectroscopic Parameters Obtained from Fitting the Temperature Dependence of $\Delta\varepsilon_{216}$ and $^3J(H^N,H^\alpha)$ of Fully Ionized DDD; (b) Thermodynamic Parameters Obtained from Fitting the Temperature Dependence of $\Delta\varepsilon_{216}$ and $^3J(H^N,H^\alpha)$ of Fully Ionized DDD

(a)							
$^3J_N(H^N,H^\alpha)$ [Hz]	J_n(pPII) [Hz]	$J_n(\beta)$ [Hz]	$^3J_c(H^N,H^\alpha)$ [Hz][a]	J_c(pPII) [Hz]	$J_c(\beta)$ [Hz]	$\Delta\varepsilon_{pPII}$ [M^{-1} cm^{-1}]	$\Delta\varepsilon_\beta$ [M^{-1} cm^{-1}]
7.22	6.38	8.48	7.62	6.34	7.64	7.18	−1.84
(b)							
χ_n(pPII)	ΔG_n [kJ/mol]	χ_c(pPII)	ΔG_c [kJ/mol]	ΔH_n [kJ/mol]	ΔH_c [kJ/mol]	ΔS_n [J/mol·K]	ΔS_c [J/mol·K]
0.59	−0.96	0.02	10.0	−11.2	−12.0	−34.6	−73.8

i = 2 and 3 for the central and the C-terminal, respectively) in the peptide.

In order to achieve consistency with the above vibrational analysis, the conformational ensemble obtained for the central residue in DDD was used to calculate the (a) average $^3J(H^N,H^\alpha)$ values of the pPII and aβt subensembles by means of eqs 1 and 3 and (b) the room-temperature (T_R) value $\Delta G_2(T_R)$ of the average Gibbs energy difference between these ensembles by using

$$\Delta G_2 = -RT_R \cdot \ln\left(\frac{\chi_\beta}{\chi_{pPII}}\right) \tag{8}$$

which could then be used to relate ΔH_2 and ΔS_2 by

$$\Delta S_2 = \frac{\Delta H_2 - \Delta G_2(T_R)}{T_R} \tag{9}$$

so that

$$\Delta G_2 = \Delta H_2 \cdot \left(1 - \frac{T}{T_R}\right) + \Delta G_2(T_R) \tag{10}$$

was obtained as the equation to be finally used in eq 4. Thus, we could fit $^3J_N(H^N,H^\alpha)(T)$ in Figure 12 by using only a single free parameter, namely, ΔH_2. This very restrictive procedure did not yield a fully satisfactory fit to the experimental data. This led us to slightly vary the ϕ values for the pPII and aβt distributions until modified $J_{pPII,N}$ and $J_{\beta,N}$ values allowed a satisfactory fitting of $^3J_N(H^N,H^\alpha)(T)$. For all of these variations, we made sure that the experimentally obtained room-temperature coupling constant was reproduced. We then used these new ϕ values to recalculate the amide I′ band profiles (Figure 9), which still led to a satisfactory fit of the thermodynamic experimental data, as shown in Figure 12. Thus, the combined analysis of amide I′ band profiles and $^3J(H^N,H^\alpha)(T)$ led to a more precise determination of conformational coordinates. The final values of $J_{pPII,N}$ and $J_{\beta,N}$ obtained from this procedure are 6.38 and 8.48 Hz, respectively (Table 3a). The thermodynamic parameters obtained from this analysis are listed in Table 3b. For the central residue of DDD, ΔG_2 = −0.96 kJ/mol at room temperature, with the enthalpic difference between pPII and aβt of ΔH_2 = −11.2 kJ/mol, whereas the entropy difference is ΔS_2 = −34.6J/mol·K. The small value for ΔG_2 is not surprising given that the corresponding mole fraction of the pPII conformation obtained for this residue is χ_{pPII} = 0.57. The small value for ΔG_2 at room temperature and the close proximity of the ϕ coordinates of the two distributions indicate that the Gibbs energy landscape for the central residue of DDD[i] is defined by a double well potential with a low barrier between the two minima, which gives rise to a broad distribution with a maximum between the ϕ positions of the minima, as shown in Figure 10.

The nearly temperature-independent $^3J(H^N,H^\alpha)$ values obtained for the C-terminal of ionized DDD, which vary between 7.62 and 7.63 Hz, can obviously not be reproduced with the N-terminal values for $J_{pPII,N}$ and $J_{\beta,N}$. In a first attempt to analyze the data, we still tried to reproduce the slight positive slope of $^3J_C(H^N,H^\alpha)(T)$. To this end, we assumed that the C-terminal is already predominantly in a conformation with an average $^3J(H^N,H^\alpha)$ coupling constant of 7.64 Hz. We then varied $J_{pPII,N}$ and simultaneously calculated the mole fraction of pPII with

$$\chi_{pPII,3} = \frac{J_C - J_{\beta,C}}{J_{P,C} - J_{\beta,C}} \tag{11}$$

where J_C denotes the experimental $^3J(H^N,H^\alpha)$ value.

The result was used in eq 8 to calculate $\Delta G_3(T_R)$, so that eqs 10 and 4 could then be employed to fit the $^3J_C(H^N,H^\alpha)(T)$, as shown in Figure 12. Thus, we obtained the solid line in this figure. From this fit, the corresponding ΔH_3 and ΔS_3 values were obtained (i.e., ΔH_2 = −12.0 kJ/mol and ΔS_2 = −73.83J/mol·K). All parameter values thus obtained are listed in Table 3b. The pPII mole fraction for the C-terminal residue at room temperature emerging from this procedure was χ_{pPII} = 0.02, which is associated with a Gibbs free-energy difference between pPII and aβt of ΔG_3 = 10.0 kJ/mol. This indicates that in contrast to the N-terminal, the C-terminal end of DDD[i] is nearly exclusively in the aβt conformation over the temperature range examined. The large difference in pPII content for N- and C-terminal indicates differences between the conformational distributions of these two residues of the peptide, which may reflect differences in the hydration shell surrounding each residue.

The deprotonated carboxylate group on the C-terminal end of the peptide seems to alter the chemical environment of this residue, effectively perturbing its hydration shell and removing any preference of the C-terminal for pPII formation. If one compares the individual thermodynamics for each residue, it becomes evident that while the enthalpy difference of the C-terminal residue is slightly more negative than that of the central residue (ΔH_2 = −11.2 kJ/mol and ΔH_3 = −12.0 kJ/mol), the entropy difference is much more negative for the C-terminal than that for the central residue (ΔS_2 = −34.6J/mol·K and ΔS_3 = −73.8J/mol·K). This difference accounts mostly for the large difference between ΔG_2 and ΔG_3 at room temperature.

With the thermodynamic parameters for each residue of DDD[i] thus obtained, the analysis of the $\Delta\varepsilon(T)$ data could be carried out using eq 6. The final fit to the experimental data is shown as the solid line in Figure 7. From this analysis, we

dx.doi.org/10.1021/jp2121565 | J. Phys. Chem. B 2012, 116, 5160−5171

obtain $\Delta\varepsilon_{pPII}$ = 7.18 $M^{-1}\,cm^{-1}$ and $\Delta\varepsilon_{\beta}$ = −1.84 $M^{-1}\,cm^{-1}$ (Table 3a).

It is informative to compare the above obtained thermodynamic parameters with corresponding values obtained for AAA.[55] The enthalpic differences are clearly larger for AAA than those for DDD^{i}, while AAA looks like a mirror image of DDD^{i} regarding the entropic differences. The ΔS_2 value of AAA (−79.6 J/mol·K) resembles ΔS_3 of DDD^{i}, while the ΔS_3 value of AAA (−26.3 J/mol·K) is not too different from the ΔS_2 value of DDD^{i}.

In addition to the temperature dependence of the *J* coupling constants, we also analyzed the temperature dependence of the chemical shift for each amide proton doublet in both ionized and protonated forms of DDD (Table 4). Resonance shifts of amide protons are temperature-dependent, generally with the chemical shift decreasing with increasing temperature. The temperature coefficient of this downshift is known to provide information on the interaction of the amide group with solvents capable of hydrogen bonding and hence indirectly on peptide conformation. In the so-called "random" or "statistical" coil conformations of unfolded peptides and proteins, amide protons are fully exposed to the solvent. The temperature coefficient characteristic of these random coil distributions is typically larger (more negative) then −6 ppb/K.[77] For both fully protonated and fully ionized DDD, we obtain chemical shift temperature coefficients that are slightly lower than the lower limit expected for fully solvent exposed amide protons (Table 4). For both protonation states, the C-terminal temperature coefficients are lower ($\Delta\delta_{i,C}$/K = −5.24 ppb/K and $\Delta\delta_{p,C}$/K = −4.8 ppb/K) than the N-terminal coefficients ($\Delta\delta_{i,N}$/K= −5.53 ppb/K and $\Delta\delta_{p,N}$/K= −5.63 ppb/K). Protection of the amide proton from solvent is known to cause lowered (less negative) temperature coefficients for the chemical shift.

Table 4. Chemical Shift Temperature Coefficients, $\Delta\delta$/K [ppb/K], for Both N- and C-Terminal Amide Protons of Fully Ionized and Protonated DDD

DDD residue type	temperature coefficient [ppb/K]
ionized, C-terminal	−5.24
ionized, N-terminal	−5.53
protonated, C-terminal	−4.81
protonated N-terminal	−5.63

The above chemical shift values are all indicative of some type of protection from the solvent, which could be due to weak intramolecular hydrogen bonding.[77] This is not unexpected for DDD^{p} because a substantial fraction of the obtained conformations sampled turns, which should be stabilized by intrapeptide hydrogen bonding of the N-terminal amide group with the C-terminal C═O group or of the C═O group of the central side chain with the C-terminal amide proton, However, one would not expect any type of intrapeptide hydrogen bonding for the two more extended conformations pPII and aβt of DDD^{i}. A closer inspection of the respective conformations, however, reveals a different picture. Figure 13 shows peptide structures that are the result of a geometry minimization of DDD^{i} and DDD^{p} in vacuo carried out by a DFT calculation on a B3LYP 6-31G** level of theory using the TITAN software package from Schrödinger, Inc. For these calculations, the coordinates of the obtained β-strand conformations of DDD^{i} and DDD^{p} were used as a starting point. For DDD^{i}, the procedure yielded a conformation with $(\phi,\psi)_2$ = (−106.7°,133°) and $(\phi,\psi)_3$ = (−99°,177°). The values for the central residue lie well within the conformation distribution shown in Figure 10. For the distances between the N-terminal amide proton and the nearest oxygen atom of the central residue, we obtained 1.6 Å, and the corresponding value for the C-terminal is 1.8 Å. These values are indicative of rather strong hydrogen bonding between the respective groups. Moreover, our results indicate a strong tendency of the N-terminal COO^{-} group to form a hydrogen bond with NH_3^{+}. For DDD^{p}, we obtained an optimized structure with $(\phi,\psi)_2$ = (−95°,163°) and with OH rather than the CO groups of the central and C-terminal aspartic acid side chains in close proximity to the respective amide proton, which is consistent with the absence of hydrogen bonding between amide protons and adjacent carboxylate groups in extended pPII/β-strand conformations.

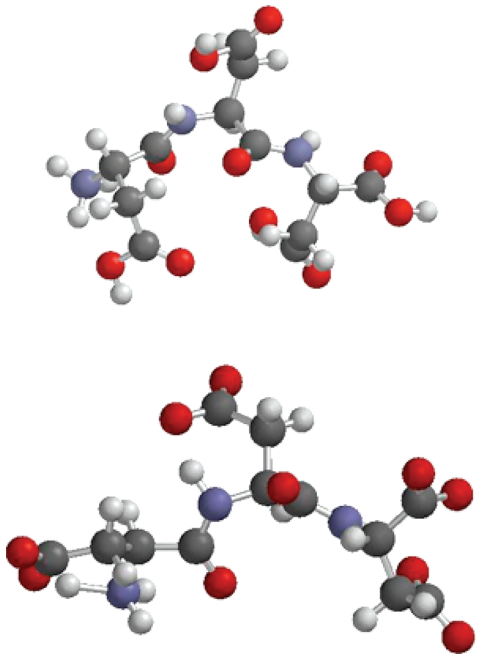

Figure 13. Conformations obtained from a DFT-based energy minimization of DDD^{p} (upper figure) and DDD^{i} (lower figure). The calculations were performed on a B3LYP 6-31G** level of theory.

Further support for suggesting hydrogen bonding in the obtained structures of DDD^{i} comes from the rather unusual amide I′ VCD signal of this peptide (Figure 9). Under normal circumstances, a mixture of pPII and aβt would give rise to a very pronounced negative couplet. The amide I′ VCD of DDD^{i}, however, exhibits a rather strong positive Cotton band, which is quite unusual. In order to account for this observation, we had to assume a rather strong magnetic transition dipole moment for the N-terminal amide I′ vibration. Interestingly, a similar phenomenon has been observed for the VCD of the $C_{\alpha}H$ stretching modes of amino acids in aqueous solution.[78] Nafie and co-workers argued that this reflects an electric asymmetric current distribution facilitated by hydrogen bonding between the terminal groups of these amino acids. Such an asymmetric current that produces a magnetic but not an electric transition dipole moment could be present in DDD^{i}. The coupling of the N-terminal amide I′ mode (CO stretch) which ND bending modes of the N-terminal ammonia group via hydrogen bonding would create a vibrational chiral entity. Nafie et at.

dx.doi.org/10.1021/jp2121565 | J. Phys. Chem. B 2012, 116, 5160−5171

suggestedthat Kuhn anisotropy ($\Delta\varepsilon_{max}/\varepsilon_{max}$) larger than 10^{-4} should be considered as an indicator for such asymmetric current distributions. In the case of DDD, the Kuhn factor is 5×10^{-5}.[78] This lower value does not argue against a asymmetric current distribution being the reason for the positive VCD signal because we cannot expect that hydrogen bonding occurs in 100% of our sample. Moreover, the proposed asymmetric current distribution does not involve the N-terminal C═O group directly so that only admixtures from, for example, $C_\alpha H$ bending modes[79] would contribute to the magnetic transition dipole moment.

Generally, we can conclude that the strong influence of pH on the conformation of DDD reflects a change of hydrogen bonding patterns rather than nearest-neighbor interactions. It is likely that this molecular switching is a peculiarity of DDD owing to its very short side chains. The question now arises as to what extent this structural flexibility might be related to the function of catalytic DDD or DxD motifs in various proteins.[51,80]

SUMMARY

In this study, we have utilized a suite of vibrational spectroscopic techniques along with UV-CD and HNMR spectrosopy to fully explore and characterize the conformational ensemble sampled by aspartic acid residues in the DDD tripeptide under both acidic and neutral conditions. The analysis of our vibrational data revealed that in its protonated form, the central residue of DDD has a distinct preference for turn-like conformations (i + 1 type I/type III β-turn ≈ 30%) typically associated with intrapeptide hydrogen bonding along the backbone. However, when the aspartic acid side chains are fully ionized, this turn-forming propensity is eliminated in preference for pPII- (45%) and β-like (55%) conformations. In addition, thermodynamic parameters obtained from a two-state analysis of the conformationally sensitive dichroism ($\Delta\varepsilon_{216\ nm}$) and $^3J(H^N,H^\alpha)$ coupling constants for ionized DDD suggest that deprotonation of the C-terminal aspartic acid and the C-terminal carboxylate group reorganizes hydrogen bonding patterns, thus inducing further preference for β-like conformations. Interestingly, we obtained NMR chemical shift temperature coefficients indicative of protection of the amide groups from solvent for both protonated and ionized DDD. For such a short peptide, we interpret this as signifying the presence of intrapeptide hydrogen bonding. Although intrapeptide hydrogen bonding is expected for the ensemble of turn conformations determined for protonated DDD, this is an unusual capability for the more extended pPII- and β-like conformations found for ionized DDD. However, closer inspection of the conformations derived from our analysis of amide I′ profiles and $^3J(H^N,H^\alpha)$ constants strongly indicates H-bonding between amide protons and the carboxylate groups of adjacent side chains even in these conformations. This type of intrapeptide hydrogen bonding has been previously shown to induce an electric asymmetric current distribution and hence a magnetic dipole moment in peptides.[78] Invoking this additional magnetic moment on the C-terminal amide vibration was necessary in our simulations in order to reproduce the positive Cotton band in the VCD profile of DDD^i. Apparently, this hydrogen bonding pattern is supported in the extended conformations sampled by DDD^i but is disrupted in favor of turn conformations and amide−carbonyl H-bonding when the side chains are protonated. Taken together, this study portrays a rather novel picture of pH-dependent conformational change and turn formation, in addition to providing early insights into the role that aspartic acid residues in general and DxD motifs in particular may play in disordered proteins.

AUTHOR INFORMATION

Corresponding Author

*Phone: 215-895-2268. Fax: 215-895-1265. E-mail: rschweitzer-stenner@drexel.edu.

Notes

The authors declare no competing financial interest.

ACKNOWLEDGMENTS

This research was supported by a NSF grant (Chem 0804492) and a REU supplement (Chem 0939972) to R.S.S.

REFERENCES

(1) Uversky, V. N.; Oldfield, C. J.; Dunker, K. A. *J. Mol. Recognit.* **2005**, *18*, 343.
(2) Uversky, V. N. *Eur. J. Biochem.* **2002**, *269*, 2.
(3) Uversky, V. N. In *Unfolded Proteins. From Denaturated to Intrinsically Disordered*; Creamer, T. P., Ed.; Nova: Nauppauge, NY, 2008.
(4) Dunker, K. A.; Obradovic, Z. *Nat. Biotechnol.* **2001**, *19*, 805.
(5) Dunker, A. K.; Cortese, M. S.; Romero, P.; Iakoucheva, I. M.; Uversky, V. N. *FEBS J.* **2005**, *272*, 5129.
(6) Dunker, A. K.; Lawson, J. D.; Brown, C. J.; Williams, R. M.; Romero, P.; Oh, J. S.; Oldfield, C. J.; Campen, A. M.; Ratliff, C. M.; Hipps, K. W.; Ausio, J.; Nissen, M. S.; Reeves, R.; Kang, C.; Kissinger, C. R.; Bailey, R. W.; Griswold, M. D.; Chiu, W.; Garner, E. C.; Obradovic, Z. *J. Mol. Graphics Modell.* **2001**, *19*, 26.
(7) Wright, P. E.; Dyson, H. J.; Lerner, R. A. *Biochemistry* **1988**, *27*, 7167.
(8) Dyson, H. J.; Rance, M.; Houghten, R. A.; Lerner, R. A.; Wright, P. E. *J. Mol. Biol.* **1988**, *201*, 161.
(9) Dyson, H. J.; Wright, P. E. *Curr. Opin. Struct. Biol.* **1993**, *3*, 60.
(10) Dyson, H. J.; Wright, P. E. *Adv. Protein Chem.* **2002**, *62*, 311.
(11) Bai, Y.; Chung, J.; Dyson, H. J.; Wright, P. E. *Protein Sci.* **2001**, *10*, 1056.
(12) Chandrasekar, K.; Profy, A. T.; Dyson, H. J. *Biochemistry* **1991**, 30.
(13) Bernado., P.; Bertoncini, C. W.; Griesinger, C.; Zweckstetter, M.; Blackledge, M. *J. Am. Chem. Soc.* **2005**, *127*, 17968.
(14) Bernado, P.; Mylonas, E.; Petoukhov, M. V.; Blackledge, M.; Svergun, D. I. *J. Am. Chem. Soc.* **2007**, *129*, 5656.
(15) Bernado, P.; Blanchard, L.; Timminis, P.; Marion, D.; Rugrok, R. W. H.; Blackledge, M. *Proc. Natl. Acad. Sci. U.S.A.* **2005**, *102*, 17002.
(16) Ohnishi, S.; Lee, A. L.; Egdell, M. H.; Shortle, D. *Biochemistry* **2004**, *43*, 4064.
(17) Dill, K. A.; Shortle, D. *Annu. Rev. Biochem.* **1991**, *60*, 795.
(18) Alexandrescu, A. T.; Abeygunawardana, C.; Shortle, D. *Biochemistry* **1994**, *33*, 1063.
(19) Mohan, A.; Oldfield, C. J.; Radivojac, P.; Vacic, V.; Cortese, M. S.; Dunker, A. K.; Uversky, V. N. *J. Mol. Biol.* **2006**, *362*, 1043.
(20) Jarvet, J.; Damberg, P.; Danielson, J.; Johansson, I.; Erikson, L. E.; Gräslund, A. *FEBS Lett.* **2003**, *555*, 371.
(21) Danielsson, J.; Jarvet, J.; Damberg, P.; Gräslund, A. *FEBS J.* **2005**, *272*, 3938.
(22) Shi, Z.; Woody, R. W.; Kallenbach, N. R. *Adv. Protein Chem.* **2002**, *62*, 163.
(23) Woody, R. W. *Adv. Biophys. Chem.* **1992**, *2*, 37.
(24) McColl, I. H.; Blanch, E. W.; Hecht, L.; Kallenbach, N. R.; Barron, L. D. *J. Am. Chem. Soc.* **2004**, *126*, 5076.
(25) Blanch, E. W.; Morozowa-Roche, L. A.; Cochran, D. A. E.; Doig, A. J.; Hecht, L.; Barron, L. D. *J. Mol. Biol.* **2000**, *301*, 553.
(26) Barron, L. D.; Hecht, L.; Blanch, E. W.; Bell, A. F. *Prog. Biophys. Mol. Biol.* **2000**, *73*, 1.

(27) Barron, L. D.; Blanch, E. W.; Hecht, L. *Adv. Protein Chem.* **2002**, *62*, 51.
(28) Mukrasch, M. D.; Markwick, P.; Biernat, J.;]von Bergen, M.; Bernado, P.; Greisinger, C.; Mandelkow, E.; Zweckstetter, M.; Blackledge, M. *J. Am. Chem. Soc.* **2007**, *129*, 5235.
(29) Bystroff, C.; Baker, D. *J. Mol. Biol.* **1998**, *281*, 565.
(30) Brahmachari, S. K.; Rajendra, S. B.; Ananthanaryanan, V. S. *Biopolymers* **1982**, *21*, 1107.
(31) Oka, M.; Montelione, G. T.; Scheraga, H. A. *J. Am. Chem. Soc.* **1984**, *106*, 7959.
(32) Montelione, G. T.; Arnold, E.; Meinwald, Y. C.; Stimson, E. R.; Denton, J. B.; Huang, S.-G.; Clardy, J.; Scheraga, H. A. *J. Am. Chem. Soc.* **1984**, *106*, 7946.
(33) Haque, T. S.; Gellman, S. H. *J. Am. Chem. Soc.* **1997**, *119*, 2303.
(34) Fuchs, P. F. J.; Bovin, A. M. J. J.; Bochicchio, B.; Pepe, A.; Alix, A. J. P.; Tamburro, A. M. *Biophys. J.* **2006**, *90*, 2745.
(35) Kieffer, B.; Mer, G.; Mann, A.; Lefévre, J.-F. *Int. J. Peptide Res.* **1994**, *44*, 70.
(36) Park, H. S.; Kim, C.; Kang, Y. K. *Biopolymers* **2002**, *63*, 298.
(37) Reed, J.; Hull, W. E.; von der Lieth, C.-W.; Kūbler, D.; Suhai, S.; Kinzel, V. *Eur. J. Biochem.* **1988**, *178*, 141.
(38) Stote, R. H.; Dejaegere, A. P.; Lefévre, J.-F.; Karplus, M. *J. Phys. Chem. B* **2000**, *104*, 1624.
(39) Pak, V. V.; Koo, m. S.; Kwon, D. Y.; Kasimova, K. D. *Chem. Nat. Prod.* **2004**, *40*, 398.
(40) Chou, P. Y.; Fasman, G. D. *Biochemistry* **1974**, *13*, 211.
(41) Zimmerman, S. S.; Scheraga, H. A. *Proc. Natl. Acad. Sci. U.S.A.* **1977**, *74*, 4126.
(42) Bondo, D.; Argos, P. *J. Mol. Biol.* **1994**, *243*, 504.
(43) Chakrabati, P.; Pal, D. *Prog. Biophys. Mol. Biol.* **2001**, *76*, 1.
(44) Duddy, W. J.; Nissink, J. M. M.; Allen, F. H.; Milner-White, E. J. *Protein Sci.* **2004**, *13*, 3051.
(45) Song, B.; Kibler, P.; Malde, A.; Kodukula, K.; Galande, A. K. *J. Am. Chem. Soc.* **2010**, *132*, 4508.
(46) Hagarman, A.; Mathieu, D.; Toal, S.; Measey, T. J.; Schwalbe, H.; Schweitzer-Stenner, R. *Chem.—Eur. J.* **2011**, *17*, 6789.
(47) Eker, F.; Griebenow, K.; Cao, X.; Nafie, L.; Schweitzer-Stenner, R. *Biochemistry* **2004**, *43*, 613.
(48) Schweitzer-Stenner, R.; Measey, T.; Kakalis, L.; Jordan, F.; Pizzanelli, S.; Forte, C.; Griebenow, K. *Biochemistry* **2007**, *46*, 1587.
(49) Hagarman, A.; Measey, T. J.; Mathieu, D.; Schwalbe, H.; Schweitzer-Stenner, R. *J. Am. Chem. Soc.* **2010**, *132*, 540.
(50) Busch, C.; Hofmann, F.; Selzer, J.; Munro, S.; Jeckel, D.; Aktories, K. *J. Biol. Chem.* **1998**, *273*, 19566.
(51) Li, J.; Rancour, D. M.; Allende, M. L.; Worth, c. A.; Darling, D. S.; Gilbert, J. B.; Menon, A. K.; Young, W. W. j. *Glycobiology* **2001**, *11*, 217.
(52) Harris, T. K.; Turner, G. J. *Life* **2002**, *53*, 85.
(53) Glasoe, P. K.; Long, F. A. *J. Phys. Chem.* **1960**, *64*, 188.
(54) Jentzen, W.; Unger, E.; Karvounis, G.; Shelnutt, J. A.; Dreybrodt, W.; Schweitzer-Stenner, R. *J. Phys. Chem.* **1995**, *100*, 14184.
(55) Toal, S.; Omidi, A.; Schweitzer-Stenner, R. *J. A. Chem. Soc.* **2011**, *133*, 12728.
(56) Schweitzer-Stenner, R. *Biophys. J.* **2002**, *83*, 523.
(57) Schweitzer-Stenner, R. *J. Phys. Chem. B* **2009**, *113*, 2922.
(58) Schweitzer-Stenner, R. *Vibr. Spectrosc.* **2006**, *42*, 98.
(59) Eker, F.; Cao, X.; Nafie, L.; Griebenow, K.; Schweitzer-Stenner, R. *J. Phys. Chem. B* **2003**, *107*, 358.
(60) Schweitzer-Stenner, R.; Measey, T. *Proc. Natl. Acad. Sci. U.S.A.* **2007**, *104*, 6649.
(61) Karplus, M. *J. Chem. Phys.* **1959**, *30*, 11.
(62) Graf, J.; Nguyen, P. H.; Stock, G.; Schwalbe, H. *J. Am. Chem. Soc.* **2007**, *129*, 1179.
(63) Oh, K.-I.; Lee, K.-K.; Park, E. K.; Kwang, G. S.; Cho, M. *Chirality* **2010**, *22*, E186.
(64) Shi, Z.; Olson, C. A.; Rose, G. D.; Baldwin, R. L.; Kallenbach, N. R. *Proc. Natl. Acad. Sci. U.S.A.* **2002**, *99*, 9190.
(65) Oh, K.-I.; Lee, K.-K.; Park, E. K.; Yoo, D.-G.; Hwang, G.-S.; Cho, M. *Chirality* **2010**, *22*, E186.
(66) Woody, R. W. *J. Am. Chem. Soc.* **2009**, *131*, 8234.
(67) Kelly, M. A.; Chellgren, B. W.; Rucker, A. L.; Troutman, J. M.; Fried, M. G.; Miller, A.; Creamer, T. P. *Biochemistry* **2001**, *2001*, 14376.
(68) Rucker, A. L.; Creamer, T. P. *Protein Sci.* **2002**, *11*, 980.
(69) Rucker, A. L.; Pager, C. T.; Campbell, M. N.; Qualls, J. E.; Creamer, T. P. *Proteins: Struct., Funct., Genet.* **2003**, *53*, 68.
(70) Eker, F.; Griebenow, K.; Schweitzer-Stenner, R. *J. Am. Chem. Soc.* **2003**, *125*, 8178.
(71) Dragomir, I.; Measey, T. J.; Hagarman, A. M.; Schweitzer-Stenner, R. *J. Phys. Chem. B* **2006**, *110*, 13235.
(72) Toal, S.; Omidi, A.; Schweitzer-Stenner, R. *J. Am. Chem. Soc.* **2011**, *133*, 12728.
(73) Schweitzer-Stenner, R.; Eker, F.; Huang, Q.; Griebenow, K. *J. Am. Chem. Soc.* **2001**, *123*, 9628.
(74) Schweitzer-Stenner, R. *J. Phys. Chem. B* **2004**, *108*, 16965.
(75) Jha, A. K.; Colubri, A.; Zaman, M. H.; Koide, S.; Sosnick, T. R.; Freed, K. F. *Biochemistry* **2005**, *44*, 9691.
(76) Sosnick, T. R. http://godzilla.uchicago.edu (2011).
(77) Dyson, H. J.; Wright, P. E. *Annu. Rev. Biophys. Biophys. Chem.* **1991**, *20*, 519.
(78) Nafie, L. A.; Oboodi, M. R.; Freedman, T. B. *J. Am. Chem. Soc.* **1983**, *105*, 7449.
(79) Mu, Y.; Stock, G. *J. Phys. Chem. B* **2002**, *106*, 5294.
(80) Heinonen, T. Y. K.; Pasternack, L.; Lindfors, K.; Breton, C.; Gastinel, L. N.; Mäki, M.; Kainulainen, H. *Biochem. Biophys. Res. Com* **2003**, *309*, 166.